



Cellular automata and Monte Carlo methods: Theory and applications in drugs and food

Marija Bezbradica, Martin Crane, Heather J. Ruskin

School of Computing, Dublin City University, Dublin, Ireland



1. INTRODUCTION

Probabilistic models (which include Monte Carlo [MC] and cellular automata [CA] among others) have attracted a huge upsurge in attention in recent years. This, in no small part, has been made possible due to ongoing increases in computing power, ever-faster networks, and cheaper memory, making so-called *Grand Challenge* problems somewhat more tractable (Ábrahám et al., 2015).

In contrast to *deterministic* models (where the relationship between quantities is known exactly), *probabilistic* models are based on the premise that, while the relationship can be modeled reasonably accurately, other components must be included to account for the variability observed in the actual data. Thus probabilistic models are statistical models, which incorporate probability distribution(s) to account for these components (Rey, 2015).

Probabilistic models are also important in that they form the basis for much work in other areas such as machine learning, artificial intelligence, and data analysis. Their formulation and solution rest on the two basic rules of probability theory, that is, the sum rule and the product rule. However, their simplicity can be deceptive; in practice all but the simplest models can become analytically and/or computationally intractable.

Developed in Los Alamos in the 1940s, MC methods make use of random sampling as a means of optimization, numerical integration, and generation of probability samples (Rubinstein, 1981). MC methods have numerous applications, ranging from the physical sciences, for example, fluid dynamics and astrophysics, through traffic modeling and statistical physics to financial analysis and business (Li, Hohne, Bortz, Bull,

& Younger, 2007; Sopasakis, 2004; Tezuka, Murata, Tanaka, & Yumae, 2005). The essence of each MC method lies in generating a set of inputs over a certain domain by sampling from a probability distribution to define a starting state. A set of deterministic computations is then performed and aggregated to obtain the “system” result. Two further classes of probabilistic models that have become increasingly popular in recent decades are CA and agent-based models (ABMs) (Clarke, 2018). Both facilitate complex systems description, built on creating elemental agents and actions that, when permuted over time and space, result in forms of aggregation or emergent behavior not found in other models or explicitly specified *ab initio*.

The structure of this chapter is as follows: the basic theory of probabilistic models is described in Section 2. Section 3 sets out probabilistic modeling with its various forms and describes practical applications in the fields from drug delivery systems in the pharmaceutical industry to nanoencapsulation in the food industry.



2. PROBABILISTIC MODELING: METHODOLOGY

2.1 Cellular automata

In computation theory, CA are an important type of discrete model used in a number of scientific fields for systems that can be conveniently represented as a regular n -dimensional grid of *cells*, each having one of a finite number of *states*. The state of each cell evolves over *discrete time*, starting from an initial state and then progressing through a series of generations, according to a fixed set of *rules* that take into account the state of the cell itself and the states of cells in its *neighborhood*.

As a type of modeling tool, CA were first discovered and described by Ulam and von Neumann in the 1940s, while working on models to describe the growth of crystals and calculate liquid motion (von Neumann, 1966). The concept involved description of the liquid as a group of small, discrete units with the motion of each unit in the flow derived according to the behavior of the neighboring units.

Perhaps the best known and most frequently used example is a two-dimensional (2D), two-state cellular automaton created by Conway in the 1970s and named the “Game of Life” (Gardner, 1970). This consists of a 2D matrix of cells which can be either alive (black) or dead (white). If

a cell has two living neighbors, its state does not change. If it has three living neighbors, it is revised. In other situations, such as four or more living neighbors (overcrowding) or a single or no neighbors (starvation), it dies. Thus the set of states includes “alive” or “dead,” and the set of rules includes various cell transition probabilities changing which govern from one state to another (Fig. 1). The initial state of the “Game of Life” can be set arbitrarily, with certain initial configurations receiving wide coverage in the scientific literature (Adachi, Lee, Peper, & Umeo, 2008; Bosch, 2000; Burguillo, 2013; Ninagawa, Yoneda, & Hirose, 1998).

Due to the “bottom-up” nature of the system description, CA make suitable and powerful tools for simulating the influence of the microscopic scale on macroscopic behavior of complex systems (Désérable, Dupont, Hellou, & Kamali-Bernard, 2011; Hoekstra, Falcone, Caiazzo, & Chopard, 2008). Thus, they have a wide application in scientific fields including traffic modeling (Burstedde, Klauck, Schadschneider, & Zittartz, 2001; Korcek, Sekanina, & Fucik, 2011; Vasic & Ruskin, 2012), bacteria growth (Margenstern, 2011), fluid dynamics (Désérable, Dupont, Hellou and Kamali-Bernard, 2011; Leon, Basurto, Martinez, & Seck-Tuoh-Mora, 2011), modeling of tumors (Patanarapeelert, Frank, & Tang, 2011), gas lattice dynamics, and many others.

CA can be divided into categories based on a number of properties, with fundamental distinctions by the type of neighborhood and nature of the rule set itself. There are two classical neighborhood types of interest in multidimensional CA: von Neumann, which considers the orthogonally adjacent cells only (four in the case of 2D automata, and six in

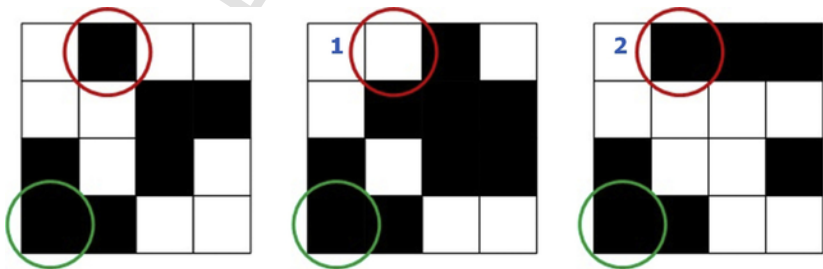


Fig. 1 An example of Conway’s “Game of Life.” Each cell can have one of two states, alive or dead, that is, black or white, respectively. As an example of dynamics: if a cell has two live neighbors (in any direction including diagonals), its state remains unchanged (*green-circled cells*). If a live cell has fewer than two live neighbors, it dies, or “starves” (*red-circled cell*, transition from initial to state 1). If a dead cell has exactly three live neighbors, it becomes live, or reproduction occurs (*red*, transition from 1 to 2).

the case of three dimensions), and Moore, which considers the entire adjacency lattice (so both orthogonal and diagonal neighbors—8 for two-dimensions, and 26 for three). While the Moore neighborhood potentially offers more realistic interactions (the CA applied to physical systems, for example), it requires more computations to evaluate the target state of the cell. Before the era of high performance computing, this disadvantage was marked for applications to complex systems, so von Neumann was generally preferred. However, with today's HPC clusters, this consideration is no longer crucial to deciding which to use, with choice governed instead by the physical realism of the problem space to be modeled (Bezbradica, Crane, & Ruskin, 2016).

Another useful division of CA concerns the nature of the state transition rules. *Deterministic* CA employ rules which are fixed and do not change over time (as in the "Game of Life," for example). In contrast, *probabilistic* CA rules may or may not be applied (managed by random number generation), and are relevant, for example, to situations where knowledge of the real system is incomplete. Stochastic CA properties are particularly useful for drug dissolution modeling, and will be extensively covered in later sections.

A final categorization of CA type is based on the order and nature of cell state updates. *Synchronous* CA apply transitions in an atomic way by calculating for the current iteration and applying changes in the next. Thus the state of the system is not dependent on the order of updates. In contrast, *asynchronous* CA apply updates in the current iteration, so that other cells are aware of the neighbor state change immediately.

2.2 Agent-based modeling

ABMs (also referred to as *multiagent systems*) present a natural extension of the CA approach. CA can be viewed as a way to model physical system dynamics by "passively" propagating a change through the modeled system by influencing a neighboring cell state. Agents provide "active" dynamism, representing independent physical entities that individually progress from cell to cell in a single iteration and are thus better suited for describing active processes, such as drug diffusion. Including a new feature in an existing CA, however, introduces additional computational requirements, and requires good code optimization and, usually, parallel reimplementations of the model (Perrin, 2008). Neverthe-

less, gains are significant. The resulting models permit large-scale simulations and inclusion of various localized effects.

ABMs are a model in which the key unit of abstraction is an *independent entity* (an agent) that has both spatial and temporal positioning. The generally accepted properties for an intelligent agent (there being no unique definition) are given by the following (Wooldridge & Jennings, 1995):

- *Autonomy*: acting without intervention with some control over its actions and the internal state.
- *Social behavior*: interacting with other agents through a specific language.
- *Reactivity*: ability to see part of its environment and change its behavior according to the environment state.
- *Proactivity*: not only reactive to the environment changes but capable of taking the initiative on action, in order to satisfy identified goals.

ABMs, like CA, provide a paradigm suitable for use in a wide variety of fields. Notable examples include economics modeling (Holland & Miller, 1991), traffic congestion (Wen, 2008), biomedical systems such as the human immune system (Kim, 2009), social and other networks (Ojanen, Sijtsema, Hawley, & Little, 2010), organizational structures (An, 2012), and social behavior (Hughes, Clegg, Robinson, & Crowder, 2012), as well as medical diagnostics (Rodríguez-González, Torres-Niño, Hernández-Chan, Jiménez-Domingo, & Alvarez-Rodríguez, 2012).

The agent-based approach requires explicit reference to agent-like entities in the system. Advantages of ABMs include modeling efficiency, robustness, interoperability between existing systems, and reasonably intuitive solving of problems for which data, expertise, and control are distributed (Jennings & Sycara, 1998). The approach is thus particularly useful in the context of natural sciences, and permits reciprocity between agents and biological entities, and between real-system interactions and exchanges between agent types. ABMs implementing several agent types are referred to as *multiagent systems*. These systems provide a generic framework for model development, as noted by Perrin (2008).

Although suitable for modeling molecular diffusion processes and naturally compatible with stochastic models, ABMs have not yet made a significant impact on polymer release modeling such as drug or nanoparticle diffusion, although an example of their use is given in a seminal paper by Barat, Crane, and Ruskin (2008). In this work, we use

a subset of agent behaviors (namely *autonomy* and *reactivity*) for describing certain active processes within the modeled device. It would be of interest, however, to examine further ABM full potential in release system modeling.

2.3 MC methods

MC methods represent a large class of computational algorithms that utilize random sampling as a means of optimization, numerical integration, and generation of probability samples (important in our case). Initial MC simulations were also performed by Ulam and von Neumann in the 1940s, while working for the Los Alamos National Laboratory.

There are two broad method groups for MC modeling. *Direct* methods use probabilistic distribution sampling for setting the initial spatial properties of the model as well the state of the modeled entities (cells, flows, agents, etc.). Direct deterministic or stochastic computations are then utilized for describing the evolution of such entities over time to produce the aggregated end result for the system. Conversely, *inverse* MC methods utilize the sampling process to try to derive the unknown but feasible distributions for model parameters, from which the known aggregated result was obtained. In other words, *direct* models start from a known initial state and attempt to derive the end result, while *inverse* methods start with a known set of one or more end results and try to determine the possible, but unknown, initial states.



3. POLYMER RELEASE THEORY AND PROBABILISTIC MODELS

The main underlying phenomena responsible for release of an active agent or a substance from food nanocapsules or pharmaceutical systems are fundamentally the same, and involve polymer erosion and diffusion mechanisms. Therefore, in this section, we focus on the fundamental polymer release theories used across both fields and review the various probabilistic modeling approaches available in order to compare advantages and disadvantages against more traditional, mechanistic, and differential equation-based approaches. Representative equations and theory, described here, provide a basis for all main polymer release modeling approaches to date, irrespective of the model type.

3.1 Important polymer release phenomena

In order to choose or develop an appropriate release model, it is of fundamental importance to understand the underlying mechanisms of polymer release (Kaunisto, Marucci, Borgquist, & Axelsson, 2011). The key physical phenomena involved can be summarized as follows:

1. *Diffusion* represents the motion of the molecules from a region of higher concentration to one of lower concentration (i.e., flux). Diffusion is often described by Fick's laws (Higuchi, 1960). In one dimension, Fick's first law can be written as:

$$J = -D \frac{\partial c(x, t)}{\partial x} \quad (1)$$

where J is the diffusion flux, D is the constant diffusion coefficient, and $\partial c(x, t)/\partial x$ is the concentration gradient.

Fick's second law predicts how diffusion causes the concentration to change with time:

$$\frac{\partial c(x, t)}{\partial t} = D \frac{\partial^2 c(x, t)}{\partial x^2} \quad (2)$$

To calculate diffusion mass transport processes in various models, Fick's second law is used in different forms, depending on the geometry of the polymer device (e.g., Cuppok et al., 2011; Kreye, Siepmann, & Siepmann, 2011; Muschert, Siepmann, Leclercq, Carlin, & Siepmann, 2009; Seidenberger, Siepmann, Bley, Maeder, & Siepmann, 2011). For example, a finite-difference approximation for determining the mass transfer rate, from cylindrical components consisting of multilayers, was applied in McMahon, Crane, Ruskin, and Crane (2003), McMahon, Crane, Ruskin, and Crane (2007), and McMahon (2008).

2. *Advection* in its general sense represents transfer of material from one region to another due to the bulk motion of the surrounding fluid. In drug release, it is a second possible mechanism involved in mass transport (in addition to diffusion), and refers to transport with specified velocity along the surface of the device (Crane, et al., 2004).
3. *Degradation* is one of the two most important processes in dissolution of polymeric devices. A widely used definition states that it is the process by which chain scission occurs (during which poly-

mer chains become monomers^a and oligomers^b). Monomers and oligomers have the ability to break down and therefore dissolve easily (Göpferich, 1996).

4. *Erosion* is a consequence of degradation and represents the loss of material from a polymer. It is an important parameter because it determines the release rate of the substance encapsulated by the polymer (Lao, Peppas, Boey, & Venkatraman, 2011; Siepmann & Göpferich, 2001). When a polymer erodes, it leaves space for the substance to be released from the device or for water ingress. Two types of erosion are defined as follows (Langer & Peppas, 1983; von Burkersroda, Schedl, & Göpferich, 2002):
 - *Surface erosion* is a homogeneous process and represents the stage during which the size of the device decreases while preserving its shape; the device loses material only from its surface (Figs. 2 and 3).
 - *Bulk erosion* is a heterogeneous process, with material being lost from the whole device, although the device dimensions remain unchanged as the polymer erosion occurs throughout (Fig. 2). For instance, surface eroding polymers like polylactide (PLA) are often used with a copolymer such as polylactic-co-glycolic acid (PLGA) to achieve bulk erosion. PLGA is a bioerodible polymer and is therefore often used in controlled release.
5. *Swelling* represents a process driven by the disentanglement and diffusion of individual polymer chains from nonhydrated polymer material, caused by solvent intake (Braidó, 2011; Kimber, Kazarian, & Štěpánek, 2012). It occurs as a response to changes in environment acidity or temperature conditions (Gehrke & Cussler, 1989). During this process, polymer chains transition from a state of low chain motion (glassy) to one of a higher motion (rubbery). This occurs until thermodynamic equilibrium (relaxation) of the chains is achieved (Lee & Peppas, 1987). Long polymer chains disentangle and detach outwards from the main mass, causing a natural concentration gradient to form from the inside of the device outwards. At the very end of the gradient, polymer erosion becomes a dominant factor as polymer concentration is very low (Fig. 4). This

^a Monomers are the simplest units of polymer. A number of monomers form complex networks of polymer chains.

^b Oligomers are simple molecules, formed of a few monomers only.

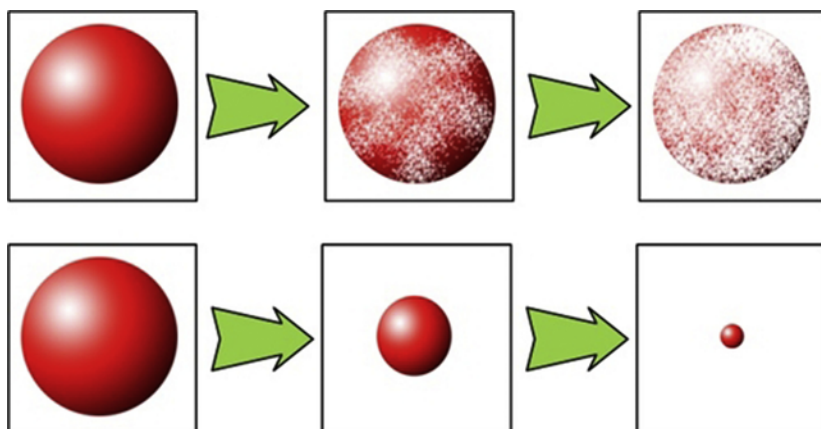


Fig. 2 Bulk erosion versus surface erosion.

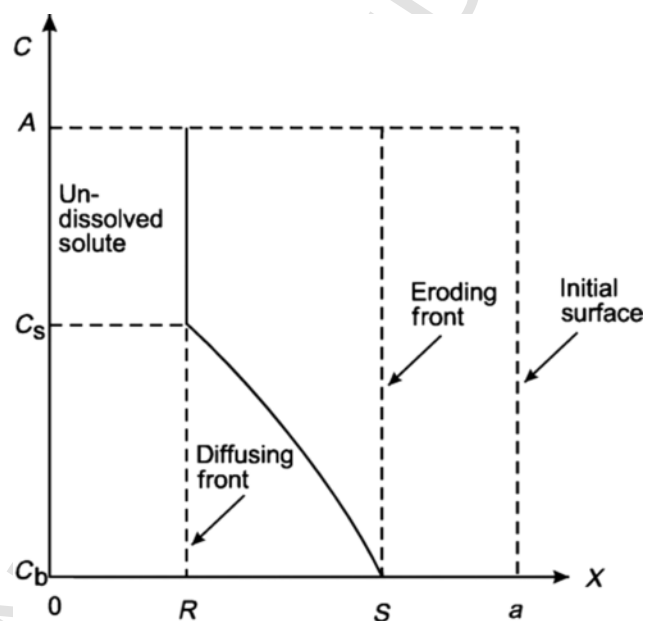


Fig. 3 General schematic representation of concentration profile for surface-eroding polymers. Two key boundary layers are visible: $R(t)$, the time-dependent position of the moving diffusion front, and $S(t)$, the time-dependent position of the eroding front (Lee, 1980).

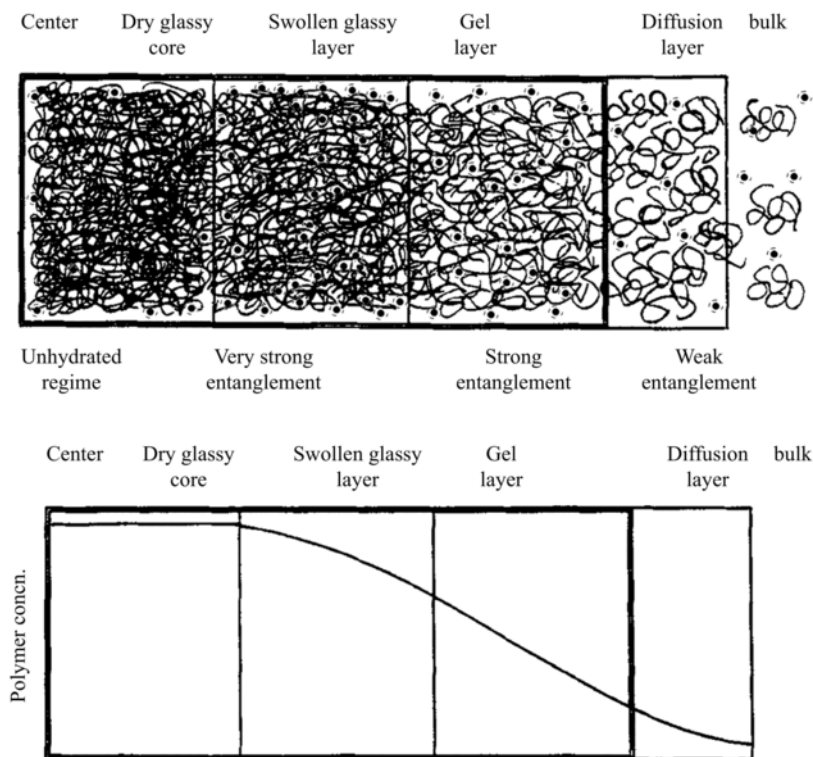


Fig. 4 (Top) Detailed schematic of polymer entanglement from nonswollen to swollen state. Within the *dry glassy core*, polymers exist in an unhydrated regime with dense network structure and low molecule mobility (left). In the *swollen glassy layer*, solvent diffusion promotes water concentrations leading to a more mobile network, and very strong chain entanglement (middle). As a result of significant swelling, fewer polymers are present in the gel layer, inducing less though still strong entanglement. Finally, in the water-rich diffusion layer, the chain entanglement becomes weak. At the gel-diffusion layer interface, chain entanglement can no longer hold polymers together, causing polymer dissolution to take place (right). Black dots represent drug particles diffusing from a nondissolved to a highly dissolved state. (Bottom) Polymer concentration profile equivalent to the top scheme. The space defined by the double lines represents the undissolved matrix. (Adapted from Ju, R. T. C., Nixon, P. R., & Patel, M. V. (1995). Drug release from hydrophilic matrices. 1. New scaling laws for predicting polymer and drug release based on the polymer disentanglement concentration and the diffusion layer. *Journal of Pharmaceutical Sciences*, 84(12), 1455–1463. <https://doi.org/10.1002/jps.2600841213>.)

process essentially characterizes swelling as a polymer diffusion process, not unlike drug diffusion.

3.1.1 Fundamental modeling methods in drug delivery

When considering polymer release in the context of drug delivery, existing models can be classified into three broad categories. The first two are based on a *top-down* approach where the main underlying phenomena must be known in some detail. Both *mechanistic* and *empirical models* are included in this category. Models in the third category are stochastic and simulate the *probabilistic* behavior of individual particles in the system, with system effects dependent on aggregation.

3.2 Challenges posed by mechanistic and empirical models

Mechanistic models, sometimes called “phenomenological models” (Sackett & Narasimhan, 2011), use differential equations for explaining dissolution processes, providing some insight into their nature at a lab-based level. The main characteristic and advantage of such models is that they enable investigation of the physical mechanisms influencing release and, by varying the relevant parameters, can be used not only to mimic experimental conditions but also as *predictive tools*. In order to validate such predictions, two options are possible: (i) comparison of modeling results with experimental data; and (ii) validation of all parameter values included in the model (as these have physical significance; Kaunisto., Kaunisto, Marucci, Borgquist and Axelsson, 2011). Another important advantage of using these models is that good matches with experiments can be obtained since equations are developed to describe accurately the underlying phenomena for a specific drug formulation. However, this is also the main disadvantage, as considerable initial knowledge of important properties is required, either from the manufacturing process itself or as determined by calculation. Therefore, a major consideration is to determine the appropriate level of complexity to be reproduced, in relation to the main release rate-limiting processes (such as the boundary conditions and the main mass transport mechanism). Defining models, which accommodate these requirements is nontrivial, particularly where multiple-parameterization and fitting are essential.

Newer compounds have even more complex behavior (Barat, Ruskin, & Crane, 2006 a) so that defining all processes involved is extremely difficult, particularly if knowledge of the delivery system is incomplete, as is often the case. Thus, the main disadvantage of mechanistic methods

is their limited applicability, that is, models are based on the experimental behavior of the particular system studied, so cannot be used to predict the effects of hypothetical changes on overall system design and behavior (Kaunisto et al., 2011).

3.2.1 The principal classical equations

Noyes-Whitney equation

The earliest mathematical models, mechanistic in nature, used to describe system behavior in polymer dissolution research appeared more than a century ago (Noyes & Whitney, 1897) with the derivation of an equation to describe the dissolution of multiparticle systems (powders). The authors discovered the dissolution rate of a solid in solution to be proportional to the difference between the current concentration of the solution and the maximal concentration of the saturated solution:

$$\frac{dc}{dt} = k_{NW}(C_s - c) \quad (3)$$

where C_s is the saturation concentration, c is the concentration of the solute at time t , and k_{NW} is a constant. Since this equation follows first-order kinetics,^c k_{NW} is considered to be a first-order proportionality constant.

Later models emphasized the assumptions for which the Noyes-Whitney (N-W) equation is applicable, namely (i) a constant area available for dissolution and (ii) a constant and intense rate of stirring (Hixson & Crowell, 1931). The N-W equation is used widely in many applications, particularly to investigate the influence of the particle size distribution on dissolution profiles (Higuchi & Hiestand, 1963; Hixson & Crowell, 1931) where the complexity of the particle size effect is emphasized. In the analysis of polydisperse multisized systems (using complex reverse engineering techniques and taking into account variations of the number of particles) dissolution profiles were found to be strongly influenced by particle size distribution (de Almeida, Simões, Brito, Portugal, & Figueiredo, 1997; Simões, de Almeida, & Figueiredo, 1996). An estimation of particle size from multisized powder dissolution was published recently (Avdeef, Tsinman, Tsinman, Sun, & Voloboy, 2009) for two scenarios in which particle size either changes or remains constant during dissolution. A good historical review of applications of the N-W equation is given by Dokoumetzidis and Macheras (2006).

^c First-order kinetics describes a release proportional to the concentration of active substance.

Higuchi equation

A second important equation, empirical in nature, and used to describe controlled release is due to Higuchi (1961). Higuchi derived an equation that follows Fick's first law and relates diffusion-controlled release of drugs from nonswellable and nonbiodegradable films under perfect sink conditions, to the diffusivity and solubility^d of a drug and its initial concentration. With increasing drug solubility, drug release occurs as a linear function of the square root of time:

$$M_t = k_H \sqrt{t} \quad (4)$$

where M_t is the cumulative amount of drug released from the ointment film during time interval t and where constant k_H has a specific meaning and should not be ignored, that is,

$$k_H = A \sqrt{2c_{ini}DC_s} \quad (5)$$

where c_{ini} is the initial drug concentration and A is the surface area available for dissolution.

The Higuchi equation must be used with caution, however, since several assumptions are made: (i) the initial substance concentration in the system is much higher than its solubility, $c_{ini} \gg C_s$; (ii) the diffusivity of the substance is constant; (iii) no swelling occurs; (iv) perfect sink conditions apply; and (v) the geometry is thin film. In consequence, the equation cannot be applied readily to systems with complex release, for example, in describing biphasic release from coated formulations (Siepmann & Peppas, 2011; Siepmann & Siepmann, 2008).

Peppas equation

The last of our general equations was derived by Korsmeyer, Gurny, Doelker, Buri, and Peppas (1983) and Ritger and Peppas (1987). Adapting the Higuchi equation, the authors provided a generalization that permits application to any geometry (thin films, cylinders, and spheres), and enables the dominant nature of the release process (Fickian or non-Fickian/anomalous) to be determined. This adaptation represents the fraction of drug release M_t/M_∞ as a simple *power-law* equation:

^d Solubility is a property of a substance (the solute, e.g., drug) to be dissolved within another substance (the solvent). The amount of drug which can be dissolved in some volume is defined by the saturation concentration (C_s). This means that additional increase of drug concentration will not result in faster drug dissolution for the given volume.

$$\frac{M_t}{M_\infty} = k_p t^n \quad (6)$$

where M_t and M_∞ represent the amounts of drug released at time t and the total amount of active substance contained by the delivery system, respectively, k_p is an experimentally determined parameter, and n is an exponent that depends on the system geometry and the mass transport mechanisms (as represented in Figs. 1, 3, and 4). It can be seen from Table 1 that if the exponent n , for the case of spherical geometries, for instance, has a value of 0.43, Fickian diffusion is the leading transport process, while a value of 0.85 refers to zero-order release, that is, concentration-independent drug release. Values larger than 0.85 indicate erosion-controlled (also referred to as *Case II*) transport (Kosmidis, Rinaki, Argyrakis, & Macheras, 2003).

The Peppas generalization is used to describe the release mechanism and provides guidance on which model to use, with many authors using the *power-law* form as the basic equation. For example, Kosmidis, Rinaki, et al. (2003) used this generalization to analyze radial and axial release from cylindrical geometries, while Casas, Strusi, Jimenez-Castellanos, and Colombo (2010) analyzed the effect of shape on drug release. In recent work, swellable systems have been modeled using a probabilistic CA approach (Laaksonen, Hirvonen, & Laaksonen, 2009) and Peppas equation was used to estimate the linearity of the release for drug fractions. Even though the equation cannot fully explain all swellable systems of interest, it has proved very useful in the investiga-

TABLE 1 Values for exponent n in the Peppas equation for different geometries and analogous drug release characteristics in polymeric-controlled delivery systems.

Value of n for different geometries			Drug release mechanism
Thin film	Thin cylinder	Sphere	
$n = 0.5$	$n = 0.45$	$n = 0.43$	Fickian transport: diffusion is the leading process
$0.5 < n < 1.0$	$0.45 < n < 0.89$	$0.43 < n < 0.85$	Non-Fickian transport, anomalous behavior: interference of more than one mass release mechanism
$n = 1.0$	$n = 0.89$	$n = 0.85$	Zero-order release

tion of complex formulations, where adequate experimental data are not available. In this way, the Peppas exponent n has been used to explain the trends in different release curve phases, that is, whether these are of zero-order or anomalous (typical for swellable systems) (Laaksonen, Hirvonen and Laaksonen, , 2009).

3.3 Probabilistic models

With the development of high-performance computers, a new approach to modeling polymer release was introduced, namely probabilistic models. While these can be both mechanistic and empirical in nature, they have the advantage of using a *bottom-up* approach, simplifying representation of the system and looking at microscopic rather than macroscopic behavior. Probabilistic models use statistical techniques such as MC and CA to describe drug release properties. Moreover, these approaches are flexible, since differential equations may also be used to define specific subelements of release phenomena, but with stochastic features incorporated (Siepmann, Faisant, & Benoit, 2002).

The basic premise of probabilistic models is the assumption that we cannot always determine the precise parameter values when modeling complex systems, and that the outcomes of individual system reactions can follow stochastic as well as deterministic rules. Such models are thus applicable to systems where: (i) the complexity of the modeled device prohibits usage of differential equations due to the inherent unknowns of many-element interactions; and (ii) the design formulation of the complex device is undetermined, making derivation of analytical solutions prohibitively expensive in terms of time. In addition to this, probabilistic methods have been shown to lack neither precision nor correctness in prediction (Barat, Ruskin, & Crane, 2006 b; Laaksonen et al., 2009; Zygourakis, 1990) and thus form a promising alternative to traditional modeling.

It is useful also to mention a class of probabilistic dissolution models that are not based on discrete space simulations using MC and CA algorithms. One interesting group in particular are those that utilize the Weibull function, since this function can be applied to almost all kinds of dissolution and related release curves (Costa & Lobo, 2001; Martínez et al., 2009). In investigating drug release for which diffusion is the dominant mechanisms, Kosmidis, Argyrakakis, and Macheras (2003) used the form:

$$\frac{M_t}{M_\infty} = 1 - e^{(-at^b)} \quad (7)$$

where M_t/M_∞ is defined as for Eq. (6) and a , b are Weibull parameters.

Starting from the Higuchi equation, the authors linked the Weibull parameters to physical properties of the drug device, showing that the *scale parameter*, a , defines the time-scale of the process and depends on the diffusion coefficient, while the *shape parameter*, b , has a constant value and characterizes the curve (Kosmidis & Macheras, 2007, 2008; Villalobos, Domínguez, Ganem, Vidales, & Cordero, 2009). Furthermore, coefficient b acts as an indicator of the transport mechanism, such that its value $b < 1$, $b = 1$, or $b > 1$ implies diffusional release (parabolic curve), first-order release (exponential curve), or complex release (sigmoidal curve), respectively (Papadopoulou, Kosmidis, Vlachou, & Macheras, 2006).

The dynamics of polymer chains, as a consequence of random disordered media of monomer obstacles, was studied using *kinetic* MC simulation by Lee and Chakraborty (2002). The polymer was modeled as a chain of spherical beads within a 3D lattice divided into cells. The cell can be either occupied by a bead or not. At each MC step, the algorithm checks the chain formation and location of the beads. If a chosen bead is found to be at the end of a chain, the bond that connects it to its nearest first neighbor will be rotated to a new position through a randomly chosen angle. Otherwise, circular rotation of the bond is effected by rotating the bonds formed with the two neighboring beads. Each movement can be accepted or rejected according to the Metropolis criterion with a probability ΔU , which represents the difference in energy between the old and new chain. The authors looked at several classes of homo- and hetero-polymers and noted that above a threshold temperature, polymers bearing monomers are attracted to sites in a disordered medium and are more mobile than those with neutral or repulsive interactions. This study improved the understanding of polymer dynamics in disordered media, with behaviors analogous to the mechanism described in Fig. 4.

In delayed release systems, as a consequence of water ingress, a polymeric coating can develop cracks due to the hydrostatic pressure build-up. This phenomenon, together with osmotic pumping, has been investigated in several studies (Kaunisto et al., 2011; Marucci, Ragnarsson, Nilsson, & Axelsson, 2010).

Recently, an interesting novel algorithm was presented for simulating the radial swelling and dissolution of cylindrical tablets using the discrete element method. Each particle was allowed to absorb water and swell, pushing against its neighbors and causing an overall expansion up to the disentanglement threshold. When that threshold is reached, the polymer dissolves and the particle decreases in size. Detailed parametric studies were performed to ascertain the main factors influencing polymer dissolution, such as the water diffusion coefficient, the dissolution rate constant, and the disentanglement ratio. The model was validated against an exact numerical solution for simpler geometries, but the additional introduction of drug particles is not discussed (Kimber, Kazarian, & Štěpánek, 2011; Kimber et al., 2012).

3.3.1 Application of direct MC methods in simulating polymer release

When applied to polymer release modeling, MC methods bring several advantages. They allow simulation of dissolution problems at increased resolutions by generating natural structural variations, and using parameters that can be estimated using the relevant probability distributions. They describe the system behavior over time as a stochastic process and enable observation of certain properties of the system at individual time steps. As an example, an MC model might describe the internal location of pores within the polymer structure as random with certain distribution characteristics. Those pores can be allowed to evolve over time using random transitions to enable increase in size, from taking in polymer or drug particles, etc. A snapshot of the system state can then be obtained at any time point to determine evolved behavior.

MC methods have been variously used to take into account mechanisms underlying the rate-limiting steps in polymer release such as diffusion, swelling, and erosion. One of the first models, developed in 1993, Göpferich and Langer (1993) simulated microstructural changes in bioerodible polymers and remains a basis for all subsequent MC simulation models. In this model, the polymer matrix was represented by a 2D computational grid, divided into individual cells. Each cell/pixel corresponded to one of two possible polymer states: amorphous (with a higher likelihood of erosion) or crystalline (with a slower erosion rate). In the polymer matrix, erosion from one particular cell occurs only if that cell is in contact with a previously eroded neighbor, where MC was used to represent this erosion as a random phenomenon. The probability of erosion of an individual cell was assumed to follow a Poisson distribution

with the characteristic value for the erosion rate being greater for amorphous than for crystalline polymers. Each cell was assigned an expectation of life (distributed as a first-order Erlang distribution).

Improvements on the original model investigated additional factors influencing erosion, such as porosity and pH changes (Göpferich & Langer, 1995 a). Both mechanistic and empirical methods were used to describe release of monomers, using Fick's second law, Eq. (2), and given by:

$$\frac{\partial}{\partial t} c(x, t) \epsilon(x, t) = \frac{\partial}{\partial x} D_{eff} c(x, t) \epsilon(x, t) \frac{\partial c(x, t)}{\partial x} \quad (8)$$

where c is the concentration of the diffusant as a function of the effective diffusivity D_{eff} , and ϵ is the porosity along the diffusion pathway.

The porosity distribution was interpreted as a network of pores, modeled using a 2D grid and MC. Degradation was considered as a spontaneous process of transformation from polymer into monomer with monomer dissolution affected by pH changes and following Fick's first law. The innovation lay in keeping track of changes in the molecular weight of the polymer. The model also enabled determination of the constant rate of erosion, but not of release predictions for the incorporated drug.

Further improvements led to investigation of surface and bulk erosion from polymers (Göpferich & Langer, 1995 b), programmable release from several layers of cylindrical eroding polymers (Göpferich, 1997 a), and erosion from slow- and fast-eroding polymers (Göpferich, 1997 b). Starting from these models, many additional MC-based models for bioerodible microparticles were generated and will be discussed further (e.g., Siepmann et al., 2002).

3.3.2 CA in direct MC methods

The first use of probabilistic CA models described drug release from bioerodible pellets. Pellets, as systems, can be composed of several components of arbitrary geometry with different dissolution rates: system behavior was defined according to local relations (Zygourakis, 1990). Subsequently, CA and parallel iterations were used (Zygourakis & Markenscoff, 1996), for the design of bioerodible devices, where the transient behavior of the surface erosion system was described. As with MC models (Göpferich & Langer, 1993, 1995 a), there are two possible states of polymer cells in the computational grid for CA: amor-

phous (highly erodible) and crystalline (poorly erodible). However, Zy-gourakis and co-workers' models were not based on differential equations. Instead, simulations were used to determine the effects of intrinsic dissolution rate, drug loading, and porosity. Improvements on early models include assumptions on the cell-dissolution neighborhood, where dissolution of each solid cell depends on the number of solvent-filled neighbors. Increased solvent around the cell leads to more rapid dissolution. The authors suggested that simulations could be used for rapid screening of newer formulations and for speeding up the design process. They highlighted the advantage of the CA approach in terms of its ability to handle multicomponent systems with arbitrary geometry.

MC, together with CA, was subsequently used for setting initial conditions to investigate the behavior of a binary device system (Barat et al., 2006 a, 2006 b). The novelty of these models was that they enabled creation of pores "inside" the device, not only on the surface, and also emphasized the importance of the surrounding medium (not defined in earlier MC/CA models). The theory on USP II apparatus medium influence was due to Ramtoola and Corrigan (1987) and Healy and Corrigan (1996), who examined the influence of particle size and discovered that, in general, a higher dissolution rate occurs for increased excipient particle size. Consequently, two boundary layers were defined in the apparatus: the *concentration layer*, where advection governs mass transport and the *velocity boundary layer* (a small region around the compact), where diffusion is the main mass transport (Crane, Crane, et al., 2004; Crane, Hurley, et al., 2004; McMahon et al., 2003). In parallel work (Barat et al., 2006 a), diffusion was modeled as the sum of the set of particles that can move to a new position. Particles that pass beyond the concentration boundary layer were considered to be dissolved. Advection was modeled using the Pohlhausen equation (Crane, Crane, et al., 2004) such that if the particle concentration in the cell is higher than a defined maximum, the particles are removed by advection. Possible states of the system were defined, according to Göpferich, Karydas, and Langer (1995) and Göpferich and Langer (1995 b), but with additional update rules.

When investigating the erosion and swelling behavior from binary matrix systems, CA without MC randomization has been used as well (Laaksonen et al., 2009; Laaksonen, Laaksonen, Hirvonen, & Murtomäki, 2009). The main differences include dispensing with arbitrary lifetimes for the drug and polymer, and assuming diffusion to be based on the pure random walk, thus eliminating the need for Fick's

first law. There is no specified expectation of life, rather the diffusion coefficient and rate of disintegration are calculated. These models were developed for several types of release mechanisms: erodible matrices, diffusion through channels/pores, membrane-controlled release, and the investigation of swelling-controlled drug release. Although the models provided a new perspective, a major limitation was the restriction to 2D cylindrical geometries due to relatively small simulation space.

3.4 Probabilistic methods in the delivery of nanomaterials

3.4.1 Nanomaterials in the delivery of functional foods

Materials at the nanoscale often have particularly useful electronic, mechanical, chemical, or optical properties, and are seeing increased use in health care, energy, food, and other sectors. Nanomaterials are typically used in the targeted delivery of minerals and other bioactive ingredients for the purposes of avoiding side-effects, degradation, or in the improvement of bioavailability (Gharibzadeh & Jafari, 2017). A recent, thorough review of nanomaterial applications in dietary supplements and foods for special medical purposes has been provided by Jampilek, Kos, and Kralova (2019). The authors note that due to the widespread usage (among other factors) of supplements and special purpose foods, they are tightly regulated in many countries, for example, by the European Food Safety Authority and the U.S. Food and Drug Administration. Obviously, due to this prevalent use, it is imperative that the mechanisms and kinetics of nanoparticle delivery and penetration are known to the fullest extent. Dietary (food) supplements may contain a variety of active ingredients (e.g., vitamins, minerals, amino acids, essential fatty acids, natural products, probiotics, etc.) (Jampilek et al., 2019). Further challenges arise in that such ingredients may be banned in some countries but legally available in others (Dwyer, Coates, & Smith, 2018). Some of the more commonly used human dietary nanosupplements are shown in Fig. 5.

In order to encapsulate drugs/nutraceuticals and fortification of food products, nanostructured lipid carriers (NLCs) have been frequently employed (Babazadeh, Ghanbarzadeh, & Hamishehkar, 2017). Further, the last two decades have seen use of solid lipid nanoparticles (SLNs) for encapsulation and delivery of bioactive components (predominantly drug formulations) which are of considerable interest to the pharmaceutical industry, but recent attention has focused also on food science and technology. Conventional carrier systems used in drug delivery (and poten-

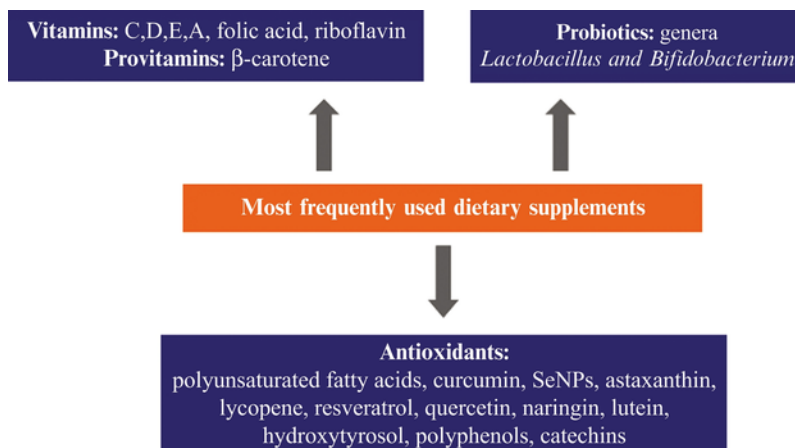


Fig. 5 Most frequently used human dietary nanosupplements. (From Jampilek, J., Kos, J., & Kralova, K. (2019). Potential of nanomaterial applications in dietary supplements and foods for special medical purposes. *Nanomaterials*, 9, 296. <https://doi.org/10.3390/nano9020296>.)

tially in food applications) are of two types: polymeric or lipidic (depending on the carrier material used in manufacture). For a recent review on SLNs, including their current and potential application in the manufacture of functional foods, see Martin-Gonzalez (2015). SLNs, however, tend to be more prevalent in applications requiring the delivery of compounds, antimicrobials, or antioxidants (Weiss et al., 2008). Although clearly promising as colloidal carriers for delivery and controlled release of the bioactive components, therefore, one difficulty for potential use of both NLCs and SLNs in functional food formulation is the limited number of emulsifiers approved by food regulators (as noted in Martin-Gonzalez, 2015). Additionally, stability issues may arise under processing for more complex products using encapsulates of both carriers, with a corresponding need for toxicology assessment.

In recent work (McClements, 2017), a delivery-by-design approach (DbD) has been proposed in order to address practical issues in encapsulation, coating, and controlled release for food (and other sectors), similar to those that arise in drug delivery systems. The author reviewed simple bioactive delivery systems, such as SLNs and NLCs, together with emulsions, polymer microparticles, and nanoparticles. For the complex delivery systems obtained by modification of properties and functionality of these systems, major structural design principles and issues are highlighted, including mechanical and physicochemical characteristics,

such as diffusion coefficient and solubility, stability issues such as pH, temperature and preoxidant levels, and so on. In addition to this, there exists an important interplay between drug and food dissolution (the so-called “food effect”; Deng et al., 2017), with the ability to predict drug disposition due to food intake involving concurrent consideration of many chemical and physiological variables (Custodio, Wu, & Benet, 2008). Further, food type and postprandial changes in the gastrointestinal tract may affect both the rate of absorption and the drug bioavailability over time. Food-drug interactions are, in consequence, actively monitored by the FDA (US), NHS (UK), and similar bodies, with some examples (such as Warfarin and grapefruit) being common and well known to the public. Very recently, Briguglio et al. (2018) reviewed bioactive compounds in food and the influence that these have on drug pharmacokinetic and pharmacodynamic profiles.

3.4.2 Nanoparticulate release mechanisms

As noted in Fathi, Donsi, and McClements (2018), the release mechanism from a nanoparticle depends on the protein composition, the nature of the bioactive molecules, the medium into which release occurs, the loading amount, and the particle geometry: moreover, different release mechanisms can occur. In a similar way to that set out above for drug release, the four principal release mechanisms from protein nanoparticles are diffusion, erosion, swelling/shrinkage, and fragmentation.

In this context too, mathematical/semianalytical models of bioactive release from nanoparticles can help in the design of encapsulation and delivery systems with desired release profiles. The semianalytical models used are substantially the same as those for drug delivery and are listed in Table 2. Properties and functionality targets for such models can be extensive (see, e.g., McClements, 2017).

3.4.3 MC methods in nanomaterials delivery

As noted in Section 1, the period of use of MC models in the design of delivery systems of dietary supplements and foods is relatively short compared to their history in drug delivery system design.

NLCs represent an improvement on micro-sized carriers in that the lipid formulation has a larger surface area designed to ensure better solubility, bioavailability, and controlled release of nanoencapsulated phenolic compounds in functional foods, where these are associated with high antioxidant capacity and benefits to human health. The impact of

TABLE 2 Kinetic models for analysis of bioactive release from nanocarriers.

Model	Equation	Model parameters	Reference
Weibull	$\frac{M_t}{M_\infty} = 1 - e^{(-at^b)}$	†	Dash, Murthy, Nath, and Chowdhury (2010)
Higuchi	$M_t = k\sqrt{t}$	★	Barzegar-Jalali et al. (2008)
Zero order	$C = kt$	★	Fathi, Mohebbi, Varshosaz, and Shahidi (2013)
First order	$C = [1 - e^{(-kt)}] \times 100$	★	Fathi et al. (2013)
Rigter-Peppas	$\frac{M_t}{M_\infty} = kt^n$	‡	Dash et al. (2010)
Reciprocal	$\left(\frac{1}{C} - 1\right) = \frac{m}{t^b}$	⊕	Mohammadi et al. (2010)
powered time			
Linear	$C = C_0 + kt$	★	Barzegar-Jalali et al. (2008)
probability			
Log-probability	$C = C_0 + k \ln t$	★	Barzegar-Jalali et al. (2008)
Hixson-Crowell	$C_0 - \sqrt[3]{1 - C} = kt$	⊗	Costa and Lobo (2001)

Parameters: † *a*, *b* scale, shape parameter; ★ *k* kinetic constant; ‡ *k* kinetic constant, *n* release exponent characterizing release mechanism; ⊗ *k*, kinetic constant incorporating surface to volume relation; ⊕ *b*, *m* shape, half-life time parameters.
Adapted from Fathi, M., Donsi, F., & McClements, D. J. (2018). Protein-based delivery systems for the nanoencapsulation of food ingredients. *Comprehensive Reviews in Food Science and Food Safety*, 17(4), 920–936. <https://doi.org/10.1111/1541-4337.12360>.

solid domain properties on the compound release rate from NLCs was investigated using MC simulations in Dan (2016). It was discovered that for the release of bioactive compounds encapsulated by solid impenetrable domains at the particle/solution interface, the only impediment to their release occurred when nanoparticle size greatly dominated domain size, even where these domains made up a large fraction of the interface. The rate of bioactives release was found to be dependent also on the solid domain geometry. Growing interest in functional foods means that the focus on phenolic compounds is ongoing, but despite their multiple bioactive properties and natural presence in plant-based foods, few marketable products currently benefit from this enrichment as there are inherent stability issues (as outlined earlier).

3.4.4 CA and ABMs in nanomaterials delivery

In distinguishing between CA and multiagent (MA) models, we noted that the former represent a way of motivating physical system dynamics by “passively” propagating change through the modeled system by influencing a neighboring cell state. However, where diffusion is the dominant mechanism, (MA) Models provide “active” dynamism, where independent physical entities are able to move from cell to cell in a single iteration; in consequence, the model formulation is better suited to the representation of the active processes found in nanomaterial delivery.

Accordingly, Zamberlan and co-authors (Zamberlan et al., 2016; Zamberlan, Kurtz, Gomes, Bordini, & Fagan, 2018) documented the construction of a simulation environment *Multi-Agent System for Polymeric Nanoparticles (MASPN)* for the production and characterization of polymeric nanoparticles as colloidal dispersions. This environment can demonstrate interactions through physical-chemical parameters, capturing Brownian motion of particles as well as attractive and repulsive behavior. The authors found that interaction of particles with the reactive environment leads to “emergent” complex behavior, which is not initially defined.

3.5 Combined ABM and CA Monte-Carlo models for controlled polymer release: A case study for drug release

Of importance for polymer-controlled release devices, which have to transition between different dissolution media, is the distinction between how each environment influences drug behavior. In mimicking the influence of acidic (pH 1.2) and enteric (pH 6.8) environments, two parameters can be utilized. The first is the relative ratio of active substance diffusion coefficients between the two environments (effectively allowing for slow-down or speed-up of the dissolution). The second is related to the presence of chemical additives, which increase the relative capability of the current environment to dissolve the target substance. As an example, active substance solubility can be low in acidic environments, but dissolution is fast with the addition of surfactants, such as sodium dodecyl sulfate.

In Bezbradica, Crane, and Ruskin (2012), the authors have modeled the following properties of the dissolution environment:

- *Dissolution rate*: that is, the speed of dissolution. The parameter defines the probability of a CyA packet dissolving in a given time

step and is directly proportional to the dissolution rate, which can be determined empirically using a variation of the Noyes-Whitney equation (3.2.1), given by:

$$D_R = \frac{AD}{h} \left(C_s - \frac{X_d}{V} \right) \quad (9)$$

where D_R is the dissolution rate, A is the surface area of the drug, h is the thickness of the boundary layer, C_s is the saturation concentration of drug in different media, X_d is the amount of dissolved drug, and V is the volume of the active dissolution media.

- *Solubility*: The maximum amount of drug that can dissolve in a defined volume of solvent. It is defined and parameterized as the dissolved drug percentage after which no more dissolution occurs due to saturation of the media. The solubility is estimated using the formula:

$$S_{tot} = k_m(C_{SURF} - CMC) \quad (10)$$

where C_{SURF} is the concentration of the surfactant, CMC is the critical micelle^e concentration of the solubilizer used (e.g., SDS surfactant used in the Sigmoid experiments has CMC of 0.008 M/L), and k_m is the molar solubilization capacity of the drug.

- *Changes in diffusivity with temperature*: Temperature changes directly influence the diffusion coefficient, so this can be partially modeled if we understand the connection between the temperature (T) and the drug diffusivity of the environment (D). For this purpose, we can use the Stokes-Einstein formula to estimate D for different T :

$$D = \frac{k_b T}{6\pi\eta r} \quad (11)$$

where η is the viscosity of the medium, k_b is the Boltzmann constant, T is the temperature of the environment, and r is the radius of the spherical particle.

The resulting model of the polymer device is then further described in terms of a discrete CA framework, satisfying the following conditions:

- Initial cell states are assigned randomly, according to a specified probability distribution, within the structural constraints of the device. (This is because the local distributions of device features,

^e Aggregation of molecules in a colloidal solution, another example of a simple delivery system (McClements, 2017).

for example, drug density or polymer composition at a given site, are unknown.)

- The different dissolution phenomena are modeled independently. (We can separately investigate the influence of polymer swelling while ignoring coating erosion and vice versa.)
- The 3D discrete space allows for models of various geometries and device compositions.
- An efficient large-scale simulation. (This is in order to explore molecular-level effects.)

The general formulation for the release device is a number of drug beads contained within a quickly erodible capsule. The models themselves simulate the dissolution of a single, idealized, drug bead represented in a 3D space, assuming its release profile to be representative of the cumulative release from all beads present in the capsule. The simulation space itself is represented by a lattice, divided into discrete cells, with each being described by a state $\Psi_{(i,j,k,t)}$ defining the aggregate condition of the bead structure at discrete space coordinates (i,j,k) and at a discrete point in time (t) . The model defines the CA rules:

$$\Phi(\sigma) : \Psi_{(i,j,k,t)} \rightarrow \Psi_{(i,j,k,t+\Delta t)} \quad (12)$$

for each cell with coordinates (i,j,k) , applied to cell state (Ψ) in order to reevaluate it after each time increment (Δt) of the simulation. When a particular rule is applied to the cell state, this is in the context of the states of all neighboring cells (σ) in the 3D space (26 in all, corresponding to a Moore neighborhood), which also determines the effect of the rule for the given cell. The rules, as applied, can thus model any distinct process that causes a change in the bead state, including drug diffusion, chain-scission of ethylcellulose polymers, erosion, or swelling of the device core. The bead itself is represented as an “idealized sphere,” consisting of a number of layers containing the drug molecules. The possible states of each cell represent different structural forms of the bead that affect the behavior of these molecules as they diffuse out of the sphere. The model defines several common cell types:

1. *Gelatine cells* (designated $|P$, as of polymer form) represent the internal structure of the bead that serves as the initial carrier of the drug.
2. *Coating cells* (designated $|C$) are used to model the coating layer of the sphere.

3. *Boundary cells* (designated $|W|$) mark the boundary of the simulation space and block any cellular transition occurring outside this.
4. *Buffer cells* (designated $|B|$) model the dissolution space around the cell.
5. *Solvent cells* (designated $|S|$) represent the internal solution inside the bead coating that is created as a consequence of dissolution of the gelatine material.

Each cell, under certain circumstances (with the exception of those in the wall layer) can hold a certain concentration of drug (C_d) represented as discrete “packets” that can model an arbitrary precision of drug volume loading $(v/v)^f$ within the cell dimensions. Between subsequent time points in the simulation (Δt), a packet can move (diffuse) to a neighboring cell. Thus, the size of the packets and the time step of the simulations are primary factors in controlling the simulation speed, and we can choose to simulate either large, bulk diffusion processes or very finely grained ones, as required.

At the beginning, each cell is initialized to a start state, depending on its location.

The coordinates of cells that satisfy the spherical equation:

$$(i - o)^2 + (j - o)^2 + (k - o)^2 - (r - d)^2 \leq 0 \quad (13)$$

(where r is the sphere radius with o the center of the sphere and d is the thickness of the coating layer) are initialized with starting gelatine state ($\Psi_{(i, j, k, 0)} = |P|$) (representing the polymer inside the bead). For each of these cells, a random number (R) between 0 and 1 is generated and compared to the drug volume (v/v) loading ratio of the sphere:

$$V_d = \frac{m_{drug} \cdot \rho_{sphere}}{m_{sphere} \cdot \rho_{drug}} \quad (14)$$

where m and ρ are the mass and the average density of the sphere and the drug itself, respectively.

If $R \leq V_d$, the cell is initialized with a number of drug packets, where this number depends on the desired resolution of the simulation. This ensures that the desired percentage of cells corresponding to the (v/v) ratio will contain drug packets. Drug diffusion is not permitted through $|P|$ cells.

^f In chemistry, volume-in-volume ratio (denoted as v/v) represents the volume of the substance relative to the total volume of the solution.

Cells that are contained outside the gelatine sphere, but within boundaries defined by the larger, coating sphere, satisfy the equation:

$$(r - d)^2 \leq (i - o)^2 + (j - o)^2 + (k - o)^2 \leq r^2 \quad (15)$$

and belong to the coating layer ($\Psi_{(i,j,k,0)} = |C$). Coating layer cells cannot contain drug packets. Cells that satisfy the boundary property ($i = 0 \vee n, j = 0 \vee n, k = 0 \vee n$) are initialized as walls: $\Psi_{(i,j,k,0)} = |W$.

All other cells are initialized to represent the buffer solution: $\Psi_{(i,j,k,0)} = |B$.

Solvent ($\Psi_{(i,j,k,t)} = |S$) cell types do not occur during model initialization, but only during cell transitions in the course of model execution.

Transition rules between cell states are represented using dimensionless ratios (one of the main advantages of CA models, as this allows comparison of processes occurring at different velocities).

The diffusion of the active substance in a governed environment is given by Fick's laws, which give the change in concentration gradient over time. Although, at macroscopic level, a given drug formulation may follow either Fickian or non-Fickian (anomalous) behavior, the assumption is made that Fick's laws always hold on a smaller scale. Movement can occur in any one of the directions in 3D space, so we assume that there exists probability of movement in any direction where there is a concentration gradient.

The model simulates the influence of Fick's laws by allowing each drug packet to have a probability (P_l) of movement to a given neighboring cell (l) with a lower drug concentration. This probability is directly proportional to the concentration gradient between two neighboring cells, that is:

$$\Delta C_l = C(i,j,k,t) - C(i^*,j^*,k^*,t) \quad (16)$$

where $C(i,j,k,t)$ and $C(i^*,j^*,k^*,t)$ represent dimensionless drug concentrations in the current and adjacent cell, respectively. The sum of all movement probabilities to permitted neighboring cells (i.e., to those for which CA rules do not prohibit movement, non- $|C$ cells) has to satisfy the law governing the sum of probabilities: $\sum_{l=0}^n P_l = 1$. Therefore, the influence of concentration differences is normalized, giving:

$$P_i = \begin{cases} \frac{\Delta C_i}{\sum_{j=0, \Delta C_j > 0}^k \Delta C_j}, & \text{if } \Delta C_i \geq 0 \\ 0, & \text{if } \Delta C_i < 0 \end{cases} \quad (17)$$

where $i \in \{0, k\}$ and k is the number of neighbors to the given cell. For certain types of cells ($|W$, $|C$ and cells where $\Delta C_i \leq 0$), P_i is assumed to be 0 by default. To summarize: according to this rule, if there exists a nonzero concentration gradient between the cell and any of its valid neighbors, there is a nonzero probability that a drug packet will move to that cell.

The speed of diffusion itself (i.e., the frequency of drug packets moving from one cell to another) is calculated using the formula defined by Laaksonen et al. (2009), which relates the simulation time step (Δt) with the diffusion coefficient (D), and the resolution of the cellular grid (a):

$$\Delta t = \frac{a^2}{4D} \quad (18)$$

The model rules are summarized as a schematic in Fig. 6.

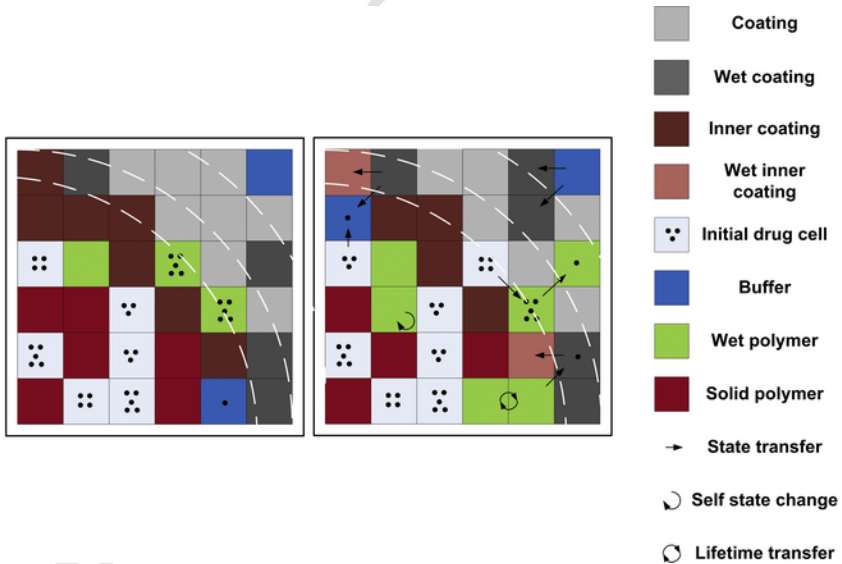


Fig. 6 A schematic representation of the CA rules for the case study model. The rules of drug diffusion and boundary erosion are displayed. *Arrows* show drug and water diffusion (*straight*), polymer erosion (*semicircular*), and polymer transfer (*swelling, circular*).

In order to categorize the release curves obtained from the models (as anomalous, Fickian, or case-2 relaxation) we use Peppas equation (6) to classify the drug dissolution, based on the parameter n and the resulting curve behavior in achieving a zero-order release rate. The parameters M and M_∞ represent the amount of drug released at time t and total amount of drug, respectively, while k_p is the kinetic constant. Values of the parameter n are obtained from resulting release curves, using linear regression methods (where n is the slope of the log-log line) of cumulative release against elapsed time, for the period during which the majority of the drug dissolution occurs.

A dimensionless Deborah number (Vrentas, Jarzebski, & Duda, 1975) can be used as an additional descriptor of the release, indicating Fickian or anomalous transport. The Deborah number is defined as:

$$De = \frac{\lambda_e}{\tau_e} = \frac{\lambda_e D_w}{\delta^2} \quad (19)$$

where λ_e represents the *characteristic relaxation time* of the polymer, τ_e is the *characteristic water diffusion time*, and δ is the gel layer thickness. Changes in the Deborah number can be estimated directly from the water diffusion and polymer swelling probabilities using the derived version of the equation, where D_w is estimated from the water diffusion probabilities, while λ_e and δ are read from the resulting simulation measurements.

Relevant simulation parameter values and their experimental references are given in Table 3. While the primary model usage was in drug dissolution, the modeling and parameter selection approach can equally be applied to other nanoscale and microscale particle delivery systems, as the nature of the released polymer is secondary to the models as long as constraints such as environment diffusivities and coating properties are accounted for.

In drawing specific parallels, similar parameterization of a nanoparticle system for food delivery would depend crucially on particle size (influencing cellular uptake), pH of the solute (also affecting size of specific nanoparticles such as gold and silver in terms of aggregation and hence stability—and influenced by coating), shape (whether circular as for beads here, or otherwise), surface charge, which is closely related to aspects of biological performance, such as solubility (and uptake), concentration (affecting toxicity), and others. The nature of coating or encapsulation can be diverse, depending on whether it is, for example, lipid and surfactant- or biopolymer-based (see Gonçalves, Martins,

TABLE 3 Model parameters used for simulation and their comparison with experimental data (Bezbradica, 2013).

Parameter	Simulation value	Experimental reference
Sphere diameter	1.8 mm	1.8 mm
D_f	$2 \times 10^{-6} \text{cm}^2/\text{s}$	0.96×10^{-6} to $5 \times 10^{-6} \text{cm}^2/\text{s}$
λ	60 min	60–120 min
Primary coat lifetime	120 min	30–120 min
P_{swelling}	0.3	0–0.5
$P_{\text{diffusion}}$	0.16	0.16
$P_{\text{water_diffusion}}$	0.01	0.01
Environment solubility	0.0	0.0
Surfactant solubility	1.0	1.0
Duration	24 h	24 h
Cell size	0.03 mm	NA
Volumetric loading	20%	20%
Mass loading	10.8%	10.8%
Primary coat thickness	0.06 mm	0.06 mm
Secondary coat thickness	0.06 mm	0.06 mm

Notes: The reference parameters were derived from available in vitro data, experimental observations, and the literature. The coating permeability was estimated based on simulated model data ranges.

Duarte, Vicente, and Pinheiro (2018) for visual representation of typical nutraceutical systems, amenable to modeling of the type described here). The food or nutraceutical matrix (e.g., for SLNs) can be similarly envisaged as clustered (or layered) or homogeneously dispersed in the excipient, and involve a bioactive-enriched core or shell and controlled release features (as also for NLC improvements in stability).

The mechanisms (Gonçalves et al., 2018) again include:

- diffusion (dependent on shape, size, structure, and composition of the delivery system, with the rate driven by the concentration gradient between the interior of the particle and its environment);
- swelling (caused by hydration and polymer relaxation, as described previously);
- erosion (due to degradation of, typically, the outer layer of the matrix and dependent on, e.g., pH, enzymes involved);
- fragmentation (matrix disruption through stress with release controlled by size and shape of particles);
- dissolution (dependent on system structure and composition and solvent type, temperature); and

- stimuli, for example, external, such as temperature change.

The number of different cell types will depend on the specific composition and structure of the delivery system and its complexity.

4. SUMMARY

Although mechanistic modeling of polymer release (applicable to drug or food nanoparticle delivery systems) has been extensively studied, the probabilistic approach is of increasing interest to researchers, as there is a growing need for improved models that can represent more elaborate release device designs while being able to accommodate more complex formulations as well as help expand theoretical knowledge in order to drive real-world applications. Using stochasticity as an integral part of such modeling has particular advantages that can help tackle such complexity, while still maintaining accurate representations of the physical characteristics underpinning release phenomena and active substance behavior, as well as the inherent dynamics. The theory review and subsequent case study show that similarity of release mechanisms together with the abstract nature of probabilistic modeling make combined CA, ABM, and MC approaches a versatile tool—set for representation of and modification testing for delivery devices with increasing levels of intricacy.

REFERENCES

- Ábrahám, E., Bekas, C., Brandic, I., Genaim, S., Johnsen, E.B., Kondov, I., Streit, A., 2015. Preparing HPC applications for exascale: Challenges. In: CoRR.(abs/1503.06974).
- Adachi, S., Lee, J., Peper, F., Umeo, H., 2008. Kaleidoscope of life: A 24-neighbourhood outer-totalistic cellular automaton. *Physica D: Nonlinear Phenomena* 237 (6), 800–817. <https://doi.org/10.1016/j.physd.2007.10.015>.
- An, L., 2012. Modeling human decisions in coupled human and natural systems: Review of agent-based models. *Ecological Modelling* 229, 25–36. <https://doi.org/10.1016/j.ecolmodel.2011.07.010>.
- Avdeef, A., Tsinman, K., Tsinman, O., Sun, N., Voloboy, D., 2009. Miniaturization of powder dissolution measurement and estimation of particle size. *Chemistry and Biodiversity* 6 (11), 1796–1811.
- Babazadeh, A., Ghanbarzadeh, B., Hamishehkar, H., 2017. Formulation of food grade nanostructured lipid carrier (NLC) for potential applications in medicinal-functional foods.. *Journal of Drug Delivery Science and Technology* 39, 50–58. <https://doi.org/10.1016/j.jddst.2017.03.001>.
- Barat, A., Crane, M., Ruskin, H.J., 2008. Quantitative multi-agent models for simulating protein release from PLGA bioerodible nano- and microspheres. *Journal of Pharma-*

- ceutical and Biomedical Analysis 48 (2), 361–368. <https://doi.org/10.1016/j.jpba.2008.02.031>.
- Barat, A., Ruskin, H.J., Crane, M., 2006. Probabilistic models for drug dissolution. Part 1. Review of Monte Carlo and stochastic cellular automata approaches. *Simulation Modelling Practice and Theory* 14 (7), 843–856. <https://doi.org/10.1016/j.simpat.2006.01.004>.
- Barat, A., Ruskin, H.J., Crane, M., 2006. Probabilistic methods for drug dissolution. Part 2. Modelling a soluble binary drug delivery system dissolving in vitro. *Simulation Modelling Practice and Theory* 14 (7), 857–873. <https://doi.org/10.1016/j.simpat.2006.03.003>.
- Barzegar-Jalali, M., Adibkia, K., Valizadeh, H., Shadbad, M.R.S., Nokhodchi, A., Omid, Y., ... Hasan, M., 2008. Kinetic analysis of drug release from nanoparticles. *Journal of Pharmacy and Pharmaceutical Sciences* 11 (1), 167–177.
- Bezradica, M. (2013). Stochastic computational modelling of complex drug delivery systems (Ph.D. thesis). Dublin City University.
- Bezradica, M., Crane, M., Ruskin, H.J., 2012. Parallelisation strategies for large scale cellular automata frameworks in pharmaceutical modelling. In: 2012 International conference on high performance computing and simulation (HPCS) pp. 223–230. <https://doi.org/10.1109/HPCSim.2012.6266916>.
- Bezradica, M., Crane, M., Ruskin, H.J., 2016. Applications of high performance algorithms to large scale cellular automata frameworks used in pharmaceutical modelling. *Journal of Cellular Automata* 11, 21–45.
- Bosch, R.A., 2000. Maximum density stable patterns in variants of Conway's game of life. *Operations Research Letters* 27 (1), 7–11. [https://doi.org/10.1016/S0167-6377\(00\)00016-X](https://doi.org/10.1016/S0167-6377(00)00016-X).
- Braido, D. (2011). *Modeling and simulation of dissolution and erosion of porous solids* (Ph.D. thesis). Graduate School, New Brunswick. <http://hdl.rutgers.edu/1782.1/rucore10001600001.ETD.000057507>.
- Briguglio, M., et al., 2018. Food bioactive compounds and their interference in drug pharmacokinetic/pharmacodynamic profiles. *Pharmaceutics* 10, 277.
- Burguillo, J.C., 2013. Playing with complexity: From cellular evolutionary algorithms with coalitions to self-organizing maps. *Computers & Mathematics With Applications* 66 (2), 201–212. <https://doi.org/10.1016/j.camwa.2013.01.020>.
- Burstedde, C., Klauck, K., Schadschneider, S., Zittartz, J., 2001. Simulation of pedestrian dynamics using a two-dimensional cellular automaton. *Physica A: Statistical Mechanics and Its Applications* 295 (3–4), 507–525. [https://doi.org/10.1016/S0378-4371\(01\)00141-8](https://doi.org/10.1016/S0378-4371(01)00141-8).
- Casas, M., Strusi, O.L., Jimenez-Castellanos, M.R., Colombo, P., 2010. Tapioca starch graft copolymers and Dome Matrix® modules assembling technology. I. Effect of module shape on drug release. *European Journal of Pharmaceutics and Biopharmaceutics* 75 (1), 42–47. <https://doi.org/10.1016/j.ejpb.2010.01.004>.
- Clarke, K.C., 2018. Cellular automata and agent-based models. In: *Handbook of regional science* Springer, pp. 1–16, Springer..
- Costa, P., Lobo, J.M.S., 2001. Modeling and comparison of dissolution profiles. *European Journal of Pharmaceutical Sciences* 13 (2), 123–133.
- Crane, M., Crane, L., Healy, A.M., Corrigan, O.I., Gallagher, K.M., McCarthy, L.G., 2004. A Pohlhausen solution for the mass flux from a multi-layered compact in

- the USP drug dissolution apparatus. *Simulation Modelling Practice and Theory* 12 (6), 397–411. <https://doi.org/10.1016/j.simpat.2004.06.004>.
- Crane, M., Hurley, N.J., Crane, L., Healy, A.M., Corrigan, O.I., Gallagher, K.M., McCarthy, L.G., 2004. Simulation of the USP drug delivery problem using CFD: Experimental, numerical and mathematical aspects. *Simulation Modelling Practice and Theory* 12 (2), 147–158. [https://doi.org/10.1016/S1569-190X\(03\)00089-3](https://doi.org/10.1016/S1569-190X(03)00089-3).
- Cuppok, Y., Muschert, S., Marucci, M., Hjaertstam, J., Siepmann, F., Axelsson, A., Siepmann, J., 2011. Drug release mechanisms from Kollicoat SR:Eudragit NE coated pellets. *International Journal of Pharmaceutics* 409 (1–2), 30–37.
- Custodio, J.M., Wu, C.-Y., Benet, L., 2008. Predicting drug disposition, absorption/elimination/transporter interplay and the role of food on drug absorption.. *Advanced Drug Delivery Reviews* 60, 717–733.
- Dan, N., 2016. Compound release from nanostructured lipid carriers (NLCs). *Journal of Food Engineering* 171, 37–43. <https://doi.org/10.1016/j.jfoodeng.2015.10.005>.
- Dash, S., Murthy, P.N., Nath, L., Chowdhury, P., 2010. Kinetic modeling on drug release from controlled drug delivery systems. *Acta Poloniae Pharmaceutica* 67, 217–223.
- de Almeida, L.P., Simões, S., Brito, P., Portugal, A., Figueiredo, M., 1997. Modeling dissolution of sparingly soluble multisized powders. *Journal of Pharmaceutical Sciences* 86 (6), 726–732. <https://doi.org/10.1021/js960417w>.
- Deng, J., Zhu, X., Chen, Z., Fan, C.H., Kwan, H.S., Wong, C.H., ... Lam, T.N., 2017. A review of food-drug interactions on oral drug absorption.. *Drugs* 77, 1833–1855.
- Désérable, D., Dupont, P., Hellou, M., Kamali-Bernard, S., 2011. Cellular automata in complex matter. *Complex Systems* 20 (1), 67–91.
- Dokoumetzidis, A., Macheras, P., 2006. A century of dissolution research: From Noyes and Whitney to the biopharmaceutics classification system. *International Journal of Pharmaceutics* 321 (1–2), 1–11. <https://doi.org/10.1016/j.ijpharm.2006.07.011>.
- Dwyer, J.T., Coates, P.M., Smith, M.J., 2018. Dietary supplements: Regulatory challenges and research resources.. *Nutrients* 10, 1–24.
- Fathi, M., Donsi, F., McClements, D.J., 2018. Protein-based delivery systems for the nanoencapsulation of food ingredients. *Comprehensive Reviews in Food Science and Food Safety* 17 (4), 920–936. <https://doi.org/10.1111/1541-4337.12360>.
- Fathi, M., Mohebbi, M., Varshosaz, J., Shahidi, F., 2013. Cellular automata modeling of hesperetin release phenomenon from lipid nanocarriers. *Food and Bioprocess Technology* 6, 3134–3142. <https://doi.org/10.1007/s11947-012-0995-2>.
- Gardner, M., 1970. Mathematical games: The fantastic combinations of John Conway's new solitaire game life. *Scientific American* 223, 120–123.
- Gehrke, S.H., Cussler, E.L., 1989. Mass transfer in pH-sensitive hydrogels. *Chemical Engineering Science* 44 (3), 559–566. [https://doi.org/10.1016/0009-2509\(89\)85032-8](https://doi.org/10.1016/0009-2509(89)85032-8).
- Gharibzadeh, S., Jafari, S.M., 2017. Nanoencapsulation of minerals. In: *Nanoencapsulation of food bioactive ingredients* pp. 333–400. <https://doi.org/10.1016/B978-0-12-809740-3.00009-X>.
- Gonçalves, R.F.S., Martins, J.T., Duarte, C.M.M., Vicente, A.A., Pinheiro, A.C., 2018. Advances in nutraceutical delivery systems: From formulation design for bioavailability enhancement to efficacy and safety evaluation. *Trends in Food Science and Technology* 78, 270–291.
- Göpferich, A., 1996. Mechanisms of polymer degradation and erosion. *Biomaterials* 17 (2), 103–114. [https://doi.org/10.1016/0142-9612\(96\)85755-3](https://doi.org/10.1016/0142-9612(96)85755-3).

- Göpferich, A., 1997. Bioerodible implants with programmable drug release. *Journal of Controlled Release* 44 (2–3), 271–281. [https://doi.org/10.1016/S0168-3659\(96\)01533-7](https://doi.org/10.1016/S0168-3659(96)01533-7).
- Göpferich, A., 1997. Erosion of composite polymer matrices. *Biomaterials* 18 (5), 397–403. [https://doi.org/10.1016/S0142-9612\(96\)00151-2](https://doi.org/10.1016/S0142-9612(96)00151-2).
- Göpferich, A., Karydas, D., Langer, R., 1995. Predicting drug release from cylindric polyanhydride matrix discs. *European Journal of Pharmaceutics and Biopharmaceutics* 42 (2), 81–87.
- Göpferich, A., Langer, R., 1993. Modeling of polymer erosion. *Macromolecules* 26, 4105–4112.
- Göpferich, A., Langer, R., 1995. Modeling monomer release from bioerodible polymers. *Journal of Controlled Release* 33 (1), 55–69.
- Göpferich, A., Langer, R., 1995. Modeling of polymer erosion in three dimensions: Rotationally symmetric devices. *American Institute of Chemical Engineers Journal* 41 (10), 2292–2299. <https://doi.org/10.1002/aic.690411012>.
- Healy, A.M., Corrigan, O.I., 1996. The influence of excipient particle size, solubility and acid strength on the dissolution of an acidic drug from two-component compacts. *International Journal of Pharmaceutics* 143 (2), 211–221. [https://doi.org/10.1016/S0378-5173\(96\)04705-9](https://doi.org/10.1016/S0378-5173(96)04705-9).
- Higuchi, T., 1960. Physical chemical analysis of percutaneous absorption process from creams and ointments. *Journal of the Society of Cosmetic Chemists* 11, 85–97.
- Higuchi, T., 1961. Rate of release of medicaments from ointment bases containing drugs in suspension. *Journal of Pharmaceutical Sciences* 50 (10), 874–875. <https://doi.org/10.1002/jps.2600501018>.
- Higuchi, W.I., Hiestand, E.N., 1963. Dissolution rates of finely divided drug powders I. Effect of a distribution of particle sizes in a diffusion-controlled process. *Journal of Pharmaceutical Sciences* 52 (1), 67–71. <https://doi.org/10.1002/jps.2600520114>.
- Hixson, A.W., Crowell, J.H., 1931. Dependence of reaction velocity upon surface and agitation. *Industrial and Engineering Chemistry* 23 (8), 923–931. <https://doi.org/10.1021/ie50260a018>.
- Hoekstra, A.G., Falcone, J.-L., Caiazzo, A., Chopard, B., 2008. Multi-scale modeling with cellular automata: The complex automata approach. In: Umeo, H., Morishita, S., Nishinari, K., Komatsuzaki, T., Bandini, S. (Eds.), *Cellular automata*. Vol. 5191, Springer, Berlin, Heidelberg, pp. 192–199. https://doi.org/10.1007/978-3-540-79992-4_25.
- Holland, J.H., Miller, J.H., 1991. Artificial adaptive agents in economic theory. *American Economic Review* 81 (2), 365–370.
- Hughes, H.P.N., Clegg, C.W., Robinson, M.A., Crowder, R.M., 2012. Agent-based modelling and simulation: The potential contribution to organizational psychology. *Journal of Occupational and Organizational Psychology* 85 (3), 487–502. <https://doi.org/10.1111/j.2044-8325.2012.02053.x>.
- Jampilek, J., Kos, J., Kralova, K., 2019. Potential of nanomaterial applications in dietary supplements and foods for special medical purposes. *Nanomaterials* 9, 296. <https://doi.org/10.3390/nano9020296>.
- Jennings, N.R., Sycara, K., 1998. A roadmap of agent research and development.. *Autonomous Agents and Multi-Agent Systems* 1, 7–38.

- Kaunisto, E., Marucci, M., Borgquist, P., Axelsson, A., 2011. Mechanistic modelling of drug release from polymer-coated and swelling and dissolving polymer matrix systems. *International Journal of Pharmaceutics* 418 (1), 54–77. <https://doi.org/10.1016/j.ijpharm.2011.01.021>.
- Kim, B.J., 2009. Prevention of falls during stairway descent in older adults. *Applied Ergonomics* 40 (3), 348–352. <https://doi.org/10.1016/j.apergo.2008.11.012>.
- Kimber, J.A., Kazarian, S.G., Štěpánek, F., 2011. A fast algorithm for mass transfer on an unstructured grid formed by DEM particles. *Powder Technology* 214 (3), 415–422. <https://doi.org/10.1016/j.powtec.2011.08.040>.
- Kimber, J.A., Kazarian, S.G., Štěpánek, F., 2012. Modelling of pharmaceutical tablet swelling and dissolution using discrete element method. *Chemical Engineering Science* 69 (1), 394–403. <https://doi.org/10.1016/j.ces.2011.10.066>.
- Korcek, P., Sekanina, L., Fucik, O., 2011. A scalable cellular automata based microscopic traffic simulation. In: *Intelligent vehicles symposium (IV)*, June 2011 IEEE pp. 13–18. <https://doi.org/10.1109/IVS.2011.5940393>.
- Korsmeyer, R.W., Gurny, K., Doelker, E., Buri, P., Peppas, N.A., 1983. Mechanisms of solute release from porous hydrophilic polymers. *International Journal of Pharmaceutics* 15 (1), 25–35. [https://doi.org/10.1016/0378-5173\(83\)90064-9](https://doi.org/10.1016/0378-5173(83)90064-9).
- Kosmidis, K., Argyrakos, P., Macheras, P., 2003. Fractal kinetics in drug release from finite fractal matrices. *Journal of Chemical Physics* 119 (12), 6373–6377. <https://doi.org/10.1063/1.1603731>.
- Kosmidis, K., Macheras, P., 2007. Monte Carlo simulations for the study of drug release from matrices with high and low diffusivity areas. *International Journal of Pharmaceutics* 343 (1–2), 166–172. <https://doi.org/10.1016/j.ijpharm.2007.05.021>.
- Kosmidis, K., Macheras, P., 2008. Monte Carlo simulations of drug release from matrices with periodic layers of high and low diffusivity. *International Journal of Pharmaceutics* 354 (1–2), 111–116.
- Kosmidis, K., Rinaki, E., Argyrakos, P., Macheras, P., 2003. Analysis of case II drug transport with radial and axial release from cylinders. *International Journal of Pharmaceutics* 254 (2), 183–188. [https://doi.org/10.1016/S0378-5173\(03\)00030-9](https://doi.org/10.1016/S0378-5173(03)00030-9).
- Kreye, F., Siepmann, F., Siepmann, J., 2011. Drug release mechanisms of compressed lipid implants. *International Journal of Pharmaceutics* 404 (1–2), 27–35.
- Laaksonen, H., Hirvonen, J., Laaksonen, T., 2009. Cellular automata model for swelling-controlled drug release. *International Journal of Pharmaceutics* 380 (1–2), 25–32.
- Laaksonen, T.J., Laaksonen, H.M., Hirvonen, J.T., Murtomäki, L., 2009. Cellular automata model for drug release from binary matrix and reservoir polymeric devices. *Biomaterials* 30 (10), 1978–1987. <https://doi.org/10.1016/j.biomaterials.2008.12.028>.
- Langer, R., Peppas, N., 1983. Chemical and physical structure of polymers as carriers for controlled release of bioactive agents: A review. *Journal of Macromolecular Science, Part C: Polymer Reviews* 23 (1), 61–126. <https://doi.org/10.1080/07366578308079439>.
- Lao, L.L., Peppas, N.A., Boey, F.Y.C., Venkatraman, S.S., 2011. Modeling of drug release from bulk-degrading polymers. *International Journal of Pharmaceutics* 418 (1), 28–41.
- Lee, P.I., 1980. Diffusional release of a solute from a polymeric matrix—Approximate analytical solutions. *Journal of Membrane Science* 7 (3), 255–275.

- Lee, P.I., Peppas, N.A., 1987. Prediction of polymer dissolution in swellable controlled-release systems. *Journal of Controlled Release* 6 (1), 207–215.
- Lee, S.-J.E., Chakraborty, A.K., 2002. Sequence dependence of polymer dynamics in quenched disordered media: Weak attraction facilitates transport. *Journal of Chemical Physics* 117 (23), 10869–10876. <https://doi.org/10.1063/1.1519838>.
- Leon, P.A., Basurto, R., Martinez, G.J., Seck-Tuoh-Mora, J.C., 2011. Complex dynamics in a hexagonal cellular automaton. In: 2011 International Conference on high performance computing and simulation (HPCS), July pp. 750–756.
- Li, D., Hohne, D., Bortz, D., Bull, J., Younger, J., 2007. Modeling bacterial clearance from the bloodstream using computational fluid dynamics and Monte Carlo simulation. *Journal of Critical Care* 22 (4), 344. <https://doi.org/10.1016/j.jcrc.2007.10.023>.
- Margenstern, M., 2011. Bacteria inspired patterns grown with hyperbolic cellular automata. In: 2011 International conference on high performance computing and simulation (HPCS), July pp. 757–763. <https://doi.org/10.1109/HPCSim.2011.5999905>.
- Martínez, L., Villalobos, R., Sánchez, M., Cruz, J., Ganem, A., Melgoza, L.M., 2009. Monte Carlo simulations for the study of drug release from cylindrical matrix systems with an inert nucleus. *International Journal of Pharmaceutics* 369 (1–2), 38–46. <https://doi.org/10.1016/j.ijpharm.2008.10.023>.
- Martin-Gonzalez, S. M. F., 2015. Solid lipid nanoparticles and applications.. Sabliov, C.M., Chen, H., Yada, R.Y. (Eds.), *Nanotechnology and functional foods: Effective delivery of bioactive ingredients*. Wiley.
- Marucci, M., Ragnarsson, G., Nilsson, B., Axelsson, A., 2010. Osmotic pumping release from ethyl-hydroxypropyl-cellulose-coated pellets: A new mechanistic model. *Journal of Controlled Release* 142 (1), 53–60. <https://doi.org/10.1016/j.jconrel.2009.10.009>.
- McClements, D.J., 2017. Delivery by design (DbD): A standardized approach to the development of efficacious nanoparticle- and microparticle-based delivery systems. *Comprehensive Reviews in Food Science and Food Safety* 17 (1), 200–219.
- McMahon, N. (2008). The mechanics of drug dissolution (Ph.D. thesis). Faculty of Engineering and Computing, School of Computing, Dublin City University. http://doras.dcu.ie/5901/nmcmahon_2008.pdf
- McMahon, N., Crane, M., Ruskin, H.J., Crane, L., 2007. The importance of boundary conditions in the simulation of dissolution in the USP dissolution apparatus. *Simulation Modelling Practice and Theory* 15 (3), 247–255.
- McMahon, N.M., Crane, M., Ruskin, H.J., Crane, L., 2003. The mechanics of drug dissolution. *Proceedings of Applied Maths and Mechanics* 3, 392–393. <https://doi.org/10.1002/pamm.200310468>.
- Mohammadi, G., Barzegar-Jalali, M., Valizadeh, H., Nazemiyeh, H., Barzegar-Jalali, A., Siahi-Shadbad, M., ... Zare, M., 2010. Reciprocal powered time model for release kinetic analysis of ibuprofen solid dispersions in oleaster powder, microcrystalline cellulose and crospovidone. *Journal of Pharmacy & Pharmaceutical Sciences* 13, 152–161. <https://doi.org/10.18433/J3JG61>.
- Muschert, S., Siepmann, F., Leclercq, B., Carlin, B., Siepmann, J., 2009. Prediction of drug release from ethylcellulose coated pellets. *Journal of Controlled Release* 135 (1), 71–79. <https://doi.org/10.1016/j.jconrel.2008.12.003>.
- Ninagawa, S., Yoneda, M., Hirose, S., 1998. 1/f fluctuation in the “Game of Life”. *Physica D: Nonlinear Phenomena* 118 (1–2), 49–52. [https://doi.org/10.1016/S0167-2789\(98\)00025-6](https://doi.org/10.1016/S0167-2789(98)00025-6).

- Noyes, A.A., Whitney, W.R., 1897. The rate of solution of solid substances in their own solutions. *Journal of the American Chemical Society* 19, 930–934.
- Ojanen, T., Sijtsma, J.J., Hawley, P.H., Little, T.D., 2010. Intrinsic and extrinsic motivation in early adolescents' friendship development: Friendship selection, influence, and prospective friendship quality. *Journal of Adolescence* 33 (6), 837–851.
- Papadopoulou, V., Kosmidis, K., Vlachou, M., Macheras, P., 2006. On the use of the Weibull function for the discernment of drug release mechanisms. *International Journal of Pharmaceutics* 309 (1–2), 44–50. <https://doi.org/10.1016/j.ijpharm.2005.10.044>.
- Patanarapeelert, K., Frank, T.D., Tang, I.M., 2011. From a cellular automaton model of tumor-immune interactions to its macroscopic dynamical equation: A drift-diffusion data analysis approach. *Mathematical and Computer Modelling* 53 (1–2), 122–130. <https://doi.org/10.1016/j.mcm.2010.07.025>.
- Perrin, D. (2008). *Multi-layered model of individual HIV infection progression and mechanisms of phenotypical expression* (Ph.D. thesis). Faculty of Engineering and Computing, School of Computing, Dublin City University. <http://doras.dcu.ie/587/1/thesis.pdf>
- Ramtoola, Z., Corrigan, O.I., 1987. Dissolution characteristics of benzoic acid and salicylic acid mixtures in reactive media. *Drug Development and Industrial Pharmacy* 13, 9–11.
- Rey, S.J., 2015. Mathematical models in geography. In: Wright, J.D. (Ed.), *International encyclopedia of the social & behavioral sciences*. Elsevier, Oxford, pp. 785–790. <https://doi.org/10.1016/B978-0-08-097086-8.72033-2>.
- Ritger, P.L., Peppas, N.A., 1987. A simple equation for description of solute release I. Fickian and non-Fickian release from non-swellable devices in the form of slabs, spheres, cylinders or discs. *Journal of Controlled Release* 5 (1), 23–36. [https://doi.org/10.1016/0168-3659\(87\)90034-4](https://doi.org/10.1016/0168-3659(87)90034-4).
- Rodríguez-González, A., Torres-Niño, J., Hernández-Chan, G., Jiménez-Domingo, E., Alvarez-Rodríguez, J.M., 2012. Using agents to parallelize a medical reasoning system based on ontologies and description logics as an application case. *Expert Systems With Applications* 39 (18), 13085–13092. <https://doi.org/10.1016/j.eswa.2012.05.093>.
- Rubinstein, R.Y., 1981. *Simulation and the Monte Carlo method*. John Wiley & Sons, Inc., New York, NY.
- Sackett, C.K., Narasimhan, B., 2011. Mathematical modeling of polymer erosion: Consequences for drug delivery. *International Journal of Pharmaceutics* 418 (1), 104–114.
- Seidenberger, T., Siepmann, J., Bley, H., Maeder, K., Siepmann, F., 2011. Simultaneous controlled vitamin release from multiparticulates: Theory and experiment. *International Journal of Pharmaceutics* 412 (1–2), 68–76.
- Siepmann, J., Faisant, N., Benoit, J.-P., 2002. A new mathematical model quantifying drug release from bioerodible microparticles using Monte Carlo simulations. *Pharmaceutical Research* 19 (12), 1885–1893. <https://doi.org/10.1023/A:1021457911533>.
- Siepmann, J., Göpferich, A., 2001. Mathematical modeling of bioerodible, polymeric drug delivery systems. *Advanced Drug Delivery Reviews* 48 (2–3), 229–247. [https://doi.org/10.1016/S0169-409X\(01\)00116-8](https://doi.org/10.1016/S0169-409X(01)00116-8).
- Siepmann, J., Peppas, N.A., 2011. Higuchi equation: Derivation, applications, use and misuse. *International Journal of Pharmaceutics* 418 (1), 6–12. <https://doi.org/10.1016/j.ijpharm.2011.03.051>.

- Siepmann, J., Siepmann, F., 2008. Mathematical modeling of drug delivery. *International Journal of Pharmaceutics* 364 (2), 328–343. <https://doi.org/10.1016/j.ijpharm.2008.09.004>.
- Simões, S., de Almeida, L., Figueiredo, M., 1996. Testing the applicability of classical diffusional models to polydisperse systems. *International Journal of Pharmaceutics* 139 (1–2), 169–176. [https://doi.org/10.1016/0378-5173\(96\)04596-6](https://doi.org/10.1016/0378-5173(96)04596-6).
- Sopasakis, A., 2004. Stochastic noise approach to traffic flow modeling. *Physica A: Statistical Mechanics and Its Applications* 342 (3–4), 741–754. <https://doi.org/10.1016/j.physa.2004.05.040>.
- Tezuka, S., Murata, H., Tanaka, S., Yumae, S., 2005. Monte Carlo grid for financial risk management. *Future Generation Computer Systems* 21 (5), 811–821. <https://doi.org/10.1016/j.future.2004.12.003>.
- Vasic, J., Ruskin, H.J., 2012. Cellular automata simulation of traffic including cars and bicycles. *Physica A: Statistical Mechanics and Its Applications* 391 (8), 2720–2729. <https://doi.org/10.1016/j.physa.2011.12.018>.
- Villalobos, R., Domínguez, A., Ganem, A., Vidales, A.M., Cordero, S., 2009. One-dimensional drug release from finite Menger sponges: In silico simulation. *Chaos, Solitons & Fractals* 42 (5), 2875–2884. <https://doi.org/10.1016/j.chaos.2009.04.007>.
- von Burkersroda, F., Schedl, L., Göpferich, A., 2002. Why degradable polymers undergo surface erosion or bulk erosion. *Biomaterials* 23 (21), 4221–4231.
- von Neumann, J., 1966. *Theory of self-reproducing automata*. University of Illinois Press, Urbana. <http://cba.mit.edu/events/03.11.ASE/docs/VonNeumann.pdf>.
- Vrentas, J.S., Jarzebski, C.M., Duda, J.L., 1975. A Deborah number for diffusion in polymer-solvent systems. *AIChE Journal* 21 (5), 894–901. <https://doi.org/10.1002/aic.690210510>.
- Weiss, J., Decker, E.A., McClements, D.J., Kristbergsson, K., Helgason, T., Awad, T., 2008. Solid lipid nanoparticles as delivery systems for bioactive food components. *Food Biophysics* 3 (2), 146–154.
- Wen, W., 2008. A dynamic and automatic traffic light control expert system for solving the road congestion problem. *Expert Systems With Applications* 34 (4), 2370–2381. <https://doi.org/10.1016/j.eswa.2007.03.007>.
- Wooldridge, M., Jennings, N.R., 1995. Intelligent agents: Theory and practice. *The Knowledge Engineering Review* 10, 115–152. <https://doi.org/10.1017/S0269888900008122>.
- Zamberlan, A., Júlia, A., Dalcin, F., Kurtz, G.C., Heitor Bordini, R., Raffin, R., Fagan, S., 2016. Simulation environment for polymeric nanoparticle: Experiment database. *Disciplinarum Scientia* 17, 429–446.
- Zamberlan, A., Kurtz, G.C., Gomes, T.L., Bordini, R.H., Fagan, S.B., 2018. A simulation environment for polymeric nanoparticles based on multi-agent systems. *Journal of Molecular Modeling* 25 (1), 5.
- Zygourakis, K., 1990. Development and temporal evolution of erosion fronts in bioerodible controlled release devices. *Chemical Engineering Science* 45 (8), 2359–2366. [https://doi.org/10.1016/0009-2509\(90\)80116-V](https://doi.org/10.1016/0009-2509(90)80116-V).
- Zygourakis, K., Markenscoff, P.A., 1996. Computer-aided design of bioerodible devices with optimal release characteristics: A cellular automata approach. *Biomaterials* 17 (2), 125–135. [https://doi.org/10.1016/0142-9612\(96\)85757-7](https://doi.org/10.1016/0142-9612(96)85757-7).

FURTHER READING

- Ju, R.T.C., Nixon, P.R., Patel, M.V., 1995. Drug release from hydrophilic matrices. 1. New scaling laws for predicting polymer and drug release based on the polymer disentanglement concentration and the diffusion layer. *Journal of Pharmaceutical Sciences* 84 (12), 1455–1463. <https://doi.org/10.1002/jps.2600841213>.